

Nanoparticle-mediated drug delivery for biofilm-associated infections

4.1 Introduction

Biofilms are complex assembly of microorganisms like bacteria, fungi, and/or other microbes that can adapt, communicate, proliferate, and spread themselves. Bacterial biofilms form when planktonic or free-floating bacterial species attach themselves to a suitable surface and begin production of characteristic extracellular polymeric substances (EPS) consisting of sugars, proteins and nucleic acids to form three-dimensional colonial network of microorganisms known as a biofilm [1]. The initial attachment of the planktonic bacteria solely depends upon the interaction between the attachment surface and microbe. According to the National Institute of Health, up to 80% of the microbial infections are caused by biofilms. The biofilms are reported to be present in 60 to 80% of chronic wound infections [2].

4.1.1 Biofilm over wounds

Wounded tissues are always at the risk of biofilm formation due to easy penetration by microbes through the compromised dermal layers, the body's first nonspecific line of defence, and disruption of the innate immune system. Wounded sites are an ideal site for biofilm formation. The necrotic tissue and cell debris provide the site for bacterial attachment and infection due to impaired host immune response at the wounded site [3]. In the initial stage of the infectious process, Gram-positive organisms such as *Staphylococcus aureus* and *Streptococcus pyogenes* are the dominant involved species. In contrast, Gram-negative microorganisms like *Escherichia coli* (*E. coli*) and *Pseudomonas aeruginosa* are only found in the later stages of the process, i.e. when a chronic wound is developed [4]. There is every possibility of the development of biofilm over the open wound if not treated appropriately and pose severe problem of

biofilm infection over the wound, as eradication of such a biofilm is very challenging and hard to achieve with regular dressings.

The cutaneous wound healing is a dynamic process in which there occurs an orderly transition from the inflammatory phase to tissue regeneration, including epithelialisation, granulation tissue formation, and angiogenesis, followed by tissue reorganisation. Microbial infection in biofilm mode targets many major inflammatory cytokines to prolonged inflammatory phase of healing in chronic wounds as damaged cells, and the immunological mediators will continue to produce pro-inflammatory cytokines leading to further injury due to generation of excess of reactive oxygen species (ROS) at the injury site [5]. The interaction between the innate immune response and the wound microbiome results in delayed-healing [3]. The implications of biofilm infected wounds are not only limited to delayed healing and financial burden but also pose the risk for persistent wound infections, especially when an implant is inserted into the body [2]. Accordingly, proper identification of microbial strains and use of tailored antibiotic medications can result in an increase in the wound healing rate up to 90% [6].

4.1.2 Biofilm-associated nosocomial infections

The biomedical devices used in the management of vital health functions are the backbone of modern medicine. Nosocomial infections associated with biofilm formation on biomedical devices also cause serious complications. Catheters made of different biomaterials like polyurethane, silicone rubber, polyvinyl chloride, polypropylene, polyethylene, Teflon etc. are the most common externally implanted medical devices (EIDs) [7]. With the advancement in the field of medical technology, a significant increase in implant-related cases of biofilm-associated infections over EIDs has

emerged as a major global health challenge [8]. Proper screening for new catheter/implant materials with desirable biocompatibility and antibacterial property for prevention of biofilm formation is still a matter of research [9]. The prevention of catheter-related infections by premature removal of catheters has led to an increase in treatment cost [10].

4.1.3 Strategies for biofilm eradication

Considerable efforts have been made to develop new antimicrobial agents for preventing biofilm-associated infections. The development of new antibiotics and widespread application of existing antibiotics has led to the growth of tolerant microorganisms either by mutation of genes or by the change in the mode of their proliferation [11]. The antibiotic resistance may involve either production of some inhibitor enzymes or by modification of the cell permeability to enhance multidrug-resistance. The genes for antibiotic resistance have been reported for transfer hereditarily in bacterial biofilms. Failure of antibiotic treatment of biofilm-related infections makes the task of treatment extremely challenging, resulting in delayed, expensive treatment or sometimes surgical removal of the implant [12].

4.1.4 Externally implanted devices (EIDs)

Applications of biomaterials in patients are very frequent these days. Catheters are the simplest biomaterial used and catheter related biofilm infections are very common. The surface of a catheter always remains in touch with biological fluids, thus provides an excellent platform for bacterial attachment and proliferation. The duration of catheterisation is a major determinant for biofilm formation on all EIDs. Nearly in 20% of the cases of health-care acquired bacterial infections in acute care facilities, and more than 50% in long term care facilities are catheter-associated urinary tract

infections [13]. Due to the lack of well-defined treatment protocol for biofilm-associated infections, it contributes significantly to patient morbidity and health-care costs.

The surface of catheter material plays a vital role in microbial attachment and propagation, still it is quite often neglected, and only a few guidelines and microbiological assessment protocols are available [14]. To overcome the problem of surface contamination, new strategies are being developed and used for surface modification and functionalisation [15]. Use of surfaces with incorporated antimicrobial property or modified with active biological nano-metals are some of the recently proposed strategies [16,17].

4.1.5 Nanoparticle-mediated drug delivery

The physico-chemical characteristics of the drug encapsulated nanoparticles (shape, size, surface charge, functional groups, and hydrophobicity) determine their interaction with bacterial biofilm colonies residing within the complex EPS matrix [18]. Drug encapsulated nanoparticles remain pristine in any biological environment only for a very short time [19]. When administered at the biofilm site, nanoparticles inevitably interact with a complex mixture of macromolecules of the biofilm to form 'biomolecular corona' that alters their surface properties, often referred to as a 'protein corona' [20,21]. The exact mechanism of protein corona formation is not yet fully elucidated. Several studies have shown that the protein corona composition and evolution are correlated to both the nanoparticle properties and the biological characteristic of the medium.

In this work, a new drug entrapped nanoparticle-based approach to prevent biofilm-associated infections has been developed. The antibiotic Gentamicin sulfate (G-

S) has been encapsulated in Eudragit RL100, which swells partially at physiological pH, thus acts as decent material for the prolonged drug release [22]. The *E. coli* bacteria are studied for their initial adhesion and ability to form mature biofilm colonies on different catheter biomaterials, namely latex rubber (Rubber catheter), silicone rubber (Foleys catheter) and polyurethane (Endotracheal tube & Enteral feeding catheter). Stainless steel (316L) plates which are commonly used in orthopaedic implants have also been tested. A comparative study has been performed for susceptibility of catheter materials to microbial adhesion and relationship of biofilm formation with their surface properties to come out with parameters to select the best material capable of resisting biofilm formation.

4.2 Literature review

Biofilm-associated infections have become the most dangerous type of virulent factor associated with infectious pathogenic microorganisms. Depending on the etiology and severity of the microbial invasion, infections can range from minor superficial to life-threatening type. Table 4.1 displays a list of major pathogenic bacteria which cause biofilm-related infections.

Table 4.1: Major pathogens involved in biofilm-associated infections [13]

Bacterial species	Biofilm infection
<i>Escherichia coli</i>	Acute and recurrent urinary tract infection, catheter-associated urinary tract infection, biliary tract infection
<i>Pseudomonas aeruginosa</i>	Chronic wound infection, cystic fibrosis lung infection, catheter-associated urinary tract infection, chronic rhinosinusitis, chronic otitis media, contact lens-related keratitis
<i>Staphylococcus aureus</i>	Chronic osteomyelitis, chronic rhinosinusitis, endocarditis, chronic otitis media, orthopaedic implants

<i>Staphylococcus epidermidis</i>	Central venous catheter, orthopaedic implants, chronic osteomyelitis
<i>Streptococcus pneumoniae</i>	Colonisation of the nasopharynx, chronic rhinosinusitis, chronic otitis media, chronic obstructive pulmonary disease
<i>Streptococcus pyogenes</i>	Colonisation of oral cavity and nasopharynx, recurrent tonsillitis

There is a high incidence of biofilm-associated infections on artificial implant devices such as catheters, orthopaedic implants, stents, contact lenses and other electronic health support devices [23]. Chronic catheter-associated biofilm infections are frequently caused by Gram-positive as well as Gram-negative bacteria [24–26]. The Food and Drug Administration (FDA) of USA has divided biomedical implants into three major categories: Class I devices that pose low levels of risk to patients and thus require minimal control; Class II devices that necessitate additional controls such as performance standards and surveillance; and Class III devices that require the most intense evaluation [1]. *Figure 4.1* displays a view of possible the sites of biofilm infections related to implanted devices and tissues.

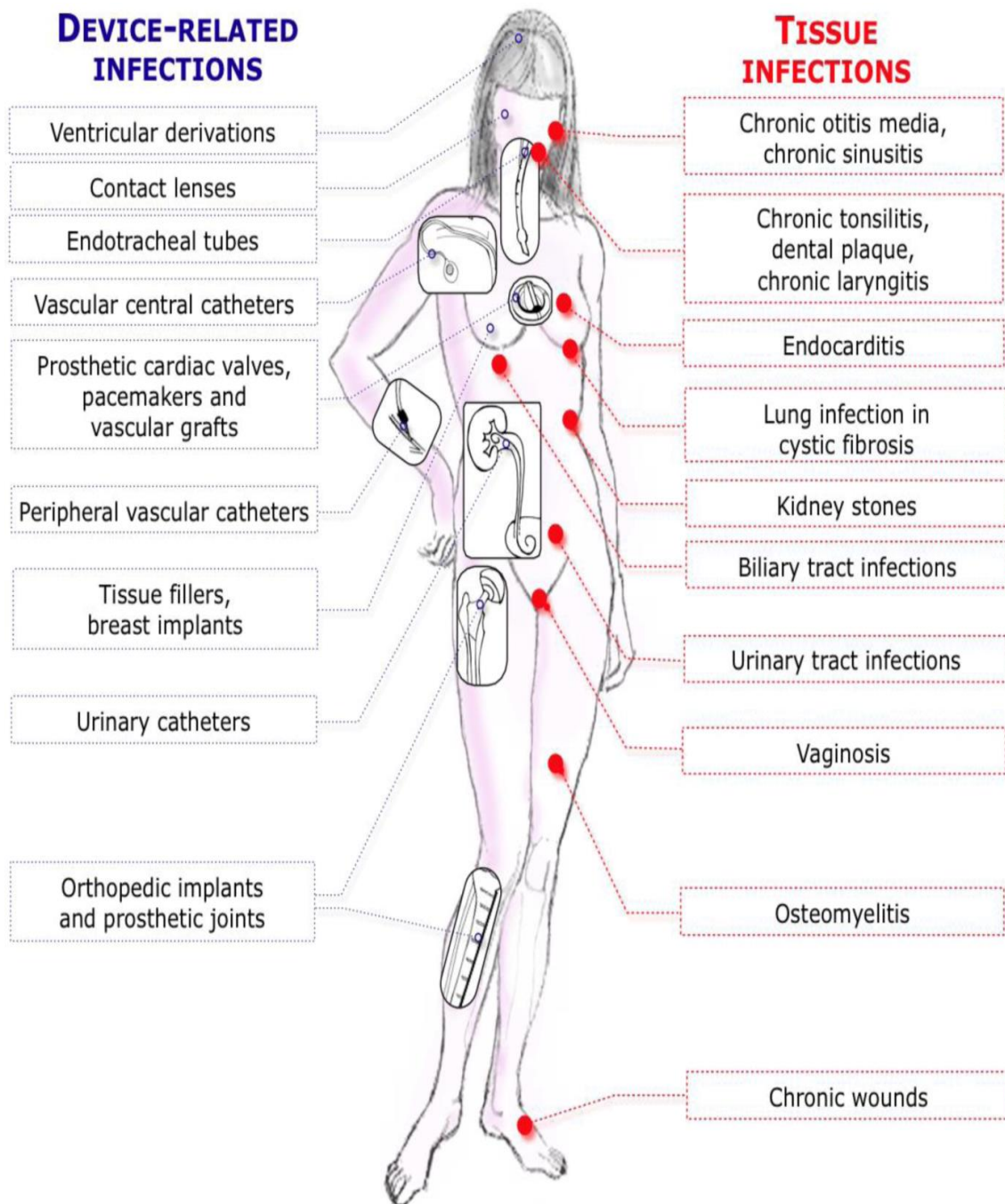


Figure 4.1: Biofilm-related infections typically found in the human body [27]

Microbial communities adhere to different surfaces using EPS microenvironment composed mainly of polysaccharides, proteinaceous molecules, lipids, mucus and some extracellular DNA (eDNA) and get embedded deep inside the EPS. Such a microenvironment improves the bacterial resistance against various factors like biocides, host defence and unfavourable environmental conditions [28,29]. The microbes in the deepest layer of biofilm are resistant to antibiotics as the EPS layers limit their exposure to antibiotics. The bacteria residing in biofilm colonies are metabolically dormant, which makes them resistant to conventional biocides sometimes thousand-fold more than the planktonic forms of the same strain [25]. Polysaccharides, proteins and eDNA help in adherence and provide mechanical strength. The antimicrobial tendency and genetic transfer governed by eDNA. Water acts as a source of ions and compounds in solution while biosurfactant and proteins help in detachment for proliferation. The virulence after detachment governed by proteins [2]. Table 4.2 lists various mechanisms by which biofilms lead to chronic disease, with associated functions and examples.

Table 4.2: Factors responsible for chronic disease and antibiotic resistance in biofilms [2]

Factors	Associated function
Exopolymeric substances or EPS	Block host detection of bacterial antigens, inflammatory response, and effect of antibiotics
Molecular messengers/host immune modulation	Inhibits host inflammatory response and wound healing to cause chronic infection, e.g. <i>P. aeruginosa</i> biofilms impair neutrophils
Genetic changes	Genetic diversity, exchange of virulence factors and antibiotic resistance genes, e.g. horizontal gene transfer, transformation
Escape behaviours	Promote new colonies establishment away from antimicrobial or immune system attack site, e.g. <i>S. viridians</i> seeding from dental plaque to endocardium
Persister phenotype	Increased resistance to antibiotics e.g. <i>E. coli</i> persister genes <i>glpD</i> , <i>glpABC</i> , <i>plsD</i>
Stress response genes	Increased resistance to antibiotics, e.g. <i>E. coli</i> <i>rpoS</i> gene
Environmental alterations	Reduction of bacterial division, e.g. maintenance of low oxygen, nutritional state microenvironment within the biofilm

4.2.1 Strategies for biofilm eradication

Several possible strategies, such as targeting the regulators, and eradicating biofilms have already been investigated [30]. Bacterial cells produce and release some signalling molecules for communication to regulate a wide variety of characteristic functions, including biofilm formation by the phenomenon of quorum sensing (QS) [31]. QS inhibitors have been used either for interrupting or degrading or modifying QS signals [32,33]. The EPS matrix-degrading enzymes have been shown to act by the degradation of polysaccharides, DNA or proteinaceous components in the biofilm

matrix [34]. Antimicrobial peptides modify the attachment, influence QS systems, and promote twitching motility [35]. Surfactants like CTAB, Tween 20, Triton X-100, rhamnolipids, etc. have also been found to be effective in lowering the surface tension to detach adherent bacterial cells leading to biofilm dispersion [6,36]. Free fatty acids tend to inhibit initial attachment by altering cell membrane function [37]. Amino acids like D-amino acid, L-tryptophan and glutamate trigger biofilm disassembly inducing biofilm dispersion [38]. Indole and its derivatives affect transcription in pathogenic *E. coli* [39]. Metal chelators act by increasing the sensitivity of cells to biocidal agents [40], nitric oxide donors induce biofilm dispersion [41], sometimes mixed treatment is also used for biofilm inhibition [42].

Currently available widely used conventional therapies to combat biofilms of species such as antibiotics, bacteriophages and QS inhibitors are inadequate for the safe and effective treatment of biofilms. Proteases easily decompose antibacterial peptides, so their efficacy got reduced [43]. Excessive application of antibiotics often produces resistance in treated bacteria resulting in multidrug-resistant bacterial species. Table 4.3 lists the advantages and disadvantages of conventionally used therapies.

Table 4.3: Advantages and disadvantages of conventional therapies against biofilm [43]

Method	Mechanism of action	Advantage	Disadvantage
Antibiotic therapy	Antibiotics with different antibacterial profiles are selected based on pathogens residing <i>in vivo</i> sites.	Targeting to the source of the disease with minimal side effects on the host cell.	(a) Unable to penetrate the EPS layer of biofilm. (b) The hypoxic environment inside the biofilm is conducive for dormant bacteria but not to the efficacy of antibiotics.
Phage therapy	The phage moves through the water channel in the biofilm to reach the bacteria in the deeper biofilm layer.	(a) Inducing depolymerisation of EPS. (b) Highly specific for specific strains.	(a) Mature biofilms have an anti-phage effect. (b) Bacteria are prone to develop resistance to phage therapy. (c) Rapid clearance by the body's immune system. (d) Need precise clinical diagnosis of bacterial species.
Quorum sensing (QS) system inhibitor	It prevents the secretion of protein effectors, destroys QS, inhibits biofilm formation, blocks signalling systems associated with virulence factor gene expression.	It does not directly target the stages necessary for normal physiological processes of the bacteria, so bacteria may develop resistance to it at a slower rate.	It cannot directly kill bacteria or inhibit bacterial growth.
Monoclonal antibody	It interferes with the formation of biofilms and promotes the disintegration of established biofilms.	Targeting to specific pathogens infections.	(a) Expensive, and it only targets common pathogens. (b) Infusion reaction.

These findings indicate that there is a need for improvement in the treatment approach towards biofilm-related infections to eradicate microbial colonies or prevent their formation completely. Recent research into biofilm treatments for wound and implant-associated infections focus on nanoparticle-mediated drug delivery, combined therapies, and implant modifications [1]. Nanoparticle-based therapies are viable approach to treat biofilm-associated infections due to the unique size-dependent chemical and physical properties of nanoparticles by virtue of their high surface area to volume ratio [19].

4.2.2 Nanoparticle-based drug delivery systems

Nanoparticle-based drug delivery systems have the potential to address the issues related to difficulties in treating biofilm infections, including low antibiotic penetration and the non-specificity [1]. It delivers antimicrobial agents for biofilm disruption and eradication. Gumus et al. in their study concluded that *Candida albicans* biofilms were eliminated by juglone nanoparticles better than free juglone and free Flucanazole [44]. Qiu et al. developed a chitosan nanoparticle-based drug delivery system encapsulating, phosphatidylcholine, and gentamicin for use against biofilms that exhibited enhanced biofilm penetration. The engulfment of the designed nanoparticles by macrophages showed negligible cytotoxicity [45]. Guo et al. developed a lipid-polymer hybrid nanoparticle loaded with linezolid for biofilm eradication [46]. Liu et al. utilised FDA approved topical ferumoxytol nanoparticles generating hydrogen peroxide and examined it for oral biofilm disruption [47].

Many studies have demonstrated the application of metal nanoparticles which are known for their antimicrobial activity and biocompatibility, to disrupt biofilms. Magnesium oxide nanoparticles have been shown to inhibit *Candida albicans* biofilm

[48]. Iron oxide nanoparticles have the potential to make it a promising option for magnetic drug-carrying biofilm inhibitor [49]. Dextran-coated iron oxide nanoparticles have been used for their selectivity towards oral biofilms by activating hydrogen peroxide for EPS break down and localised death [50]. Vasile et al. developed wound dressing based on silver nanoparticles, sodium alginate, and essential oils for enhanced antimicrobial activity [51]. Hybrid blend of silver-gold nanoparticles which generated intracellular oxidative stress and cell wall damage, were effectively used in Gram-negative and Gram-positive bacteria for biofilm reduction [52]. Mechanisms which are specifically directed towards disrupting the cellular function of bacteria or biofilms may also prove to be effective in nanoparticles based delivery systems.

The above studies demonstrate the successful application of nanoparticle-based drug delivery systems for biofilm eradication. Their application in wounds and implant-related biofilm infections may be useful to break the barrier of treating multidrug-resistant biofilms effectively. Clinical trials would be necessary to assess their efficacy and the feasibility of their large-scale production and application in health-care.

In view of above literature and knowledge gap this work has been planned with objective to study the pattern of biofilm over different surfaces and develop antibiotic encapsulated Eudragit RL100 nanoparticle mediated drug delivery system to eradicate biofilm related iatrogenic infections and wound infections. The drug delivery system was expected to eradicate the biofilm infections effectively with lower the drug dose without any side effects.

4.3 Materials and methods

4.3.1 Materials and reagents

Eudragit RL-100 was purchased from Evonik Rohm GmbH Darmstadt, gentamicin sulfate (G-S) and mannitol was purchased from Sigma-Aldrich, USA. Polyvinyl alcohol (PVA), methylene dichloride (MDC), nutrient agar, phosphate buffer saline (PBS), nutrient broth, Lysogeny broth (LB), crystal violet (CV), dimethyl sulphoxide, ethanol, disodium hydrogen phosphate, potassium dihydrogen phosphate were purchased from Himedia Laboratories Pvt. Ltd., Mumbai, India. The standard strain of *Escherichia coli* (ATCC 25922) procured from Institute of Medical Sciences, BHU, Varanasi and was used as the reference in this study. Externally implanted medical devices (EIDs)/catheters [enteral feeding catheter (Ramsons), rubber catheter, Foleys catheter (Ramsons) and stainless steel plates-(316L) (Zealmax India)] were obtained from local medical shops. All solvents and chemicals used were of analytical grade. The borosilicate glass-wares used in experiments were acid-washed and rinsed with double distilled (DD) water followed by heat sterilisation before use.

4.3.2 Biofilm formation and quantification

Biofilms were formed on the EIDs using the microtiter dish biofilm formation assay [53]. *E. coli* strain was cultured in LB broth at 37°C for 24 h, and the cell density was set at 1.5×10^8 cell/mL using a hemocytometer. 1 mL of 1.5×10^8 CFU/mL of *E. coli* suspension was added to a 2 mL capped eppendorf tube having [(0.5×0.5) cm²] EIDs and incubated at 37°C for 90 to 120 min (adhesion phase). After incubation, EIDs were washed with PBS, and then a fresh broth was added to the catheters, and subsequently incubated at 37°C for 24, 48, and 72 h for biofilm formation. Timely quantification of biofilm was done by crystal violet assay [54]. 0.5% (w/v) CV solution in DDW was

applied to the catheter pieces, and subsequently incubated for 30 minutes at room temperature. After 30 min of incubation, the blocks were rinsed thrice with PBS to remove any unbound dye. Later the CV was washed out from the bacterial biofilms over the catheter surfaces with 96% ethanol, and the resultant solution was spectrophotometrically analyzed for the absorption of the resulting violet solution at 600 nm using 96% ethanol as the blank, the absorbance corresponds to the extent of formation of biofilm [55].

4.3.3 Scanning electron microscopy (SEM)

The scanning electron microscopic (SEM) analysis was performed for determining the size of the formed nanoparticles, the sample's surface morphology of EIDs and bacterial biofilm. All the EIDs sample [(0.5 x 0.5) cm²] were pasted onto the sample holder and E-G-S nanoparticles were allowed to dry at the ambient temperature before the measurement using SEM (FEI, Quanta 200F, Japan) at an acceleration voltage of 10 kV. Lyophilized E-G-S samples were also analysed for their size and size distribution using Dynamic Light Scattering method (Particulate Systems, Nanoplus particle size analyser, Norcross Georgia, GA, USA) [56].

4.3.4 Water contact angle (WCA)

The hydrophilicity and hydrophobicity of the EID surface were evaluated by the surface contact angle measurement between the sessile water drop and EID surface. The WCA measurement for water was performed by using contact angle measuring drop shape analyser (DSA25S, KRUSS, Germany). A drop of water (20 µL) was dropped over the piece of catheter material using an automatic micro-syringe, and then static images for each surface were taken [57]. In each case, the angle was measured thrice and the average value was taken as the contact angle value of that material surface.

4.3.5 Preparation of Eudragit-RL100 nanoparticle encapsulated gentamicin sulfate (E-G-S)

Nanoparticle encapsulated G-S was prepared by the solvent displacement or nanoprecipitation technique [22]. The PVA solution of known concentration (5% w/v in 100 mL distilled water) was prepared and stirred at room temperature for 10 min to obtain a homogeneous solution. 100 mg of G-S was mixed in this solution. In a clean Erlenmeyer flask, 5 g of Eudragit RL-100 was dissolved in 100 mL of MDC and sonicated for 5 s. The G-S solution was added to the sonicated Eudragit RL-100 solution and further sonicated for 25 s to form a water-in-organic emulsion (w/o). A fresh 250 mL of PVA solution (1% w/v) was then added in water-in-organic emulsion to form water-organic-water emulsion (w-o-w) multiple emulsion. The resultant emulsion was homogenised at 15000-20000 rpm thrice to form the Eudragit RL-100 nanoparticle encapsulated drug. 250 mL of PVA (0.3% w/v) was prepared in DD water and mixed with multiple emulsion and agitated using a magnetic stirrer for 6 h at 25°C at 200 rpm to evaporate the MDC and organic solvents. To get the nanoparticle in powder form, deep-frozen samples were placed in a lyophiliser at -40°C until the dried powdered sample was obtained.

4.3.5.1 Drug entrapment efficiency

A 20 mL solution of the prepared nano-suspension was centrifuged at 18,000 rpm for 2.5 h at 10°C, using Remi C-24 cooling centrifuge. The proportion of untrapped drug was estimated by taking the absorbance of the appropriately diluted supernatant solution at 260 nm using UV-Visible Spectrophotometer (Systronics, Model 2202) against blank/control nanosuspension. By subtracting the amount of G-S in supernatant

from the initial amount of the G-S taken, entrapment efficiency of nanoparticle was calculated using the equation 4.1;

$$\text{Entrapment efficiency} = \frac{\text{Amount of drug entrapped in nanoparticle}}{\text{Initial amount of drug used}} \times 100 \quad (4.1)$$

Amount of drug entrapped = Initial amount of drug used – Drug present in the supernatant

4.3.5.2 *In vitro* gentamicin sulfate release kinetic study

The *in vitro* drug release kinetics of the formed nanoparticle was studied by the static Franz diffusion cell [58]. A dialysis membrane made of cellulose acetate of 25 mm diameter was placed at the terminal portion of the donor compartment. A 10 mL portion of the nanosuspension with the drug was placed into the donor compartment to act as a source. The receptor compartment was filled with 90 mL of 0.2 M phosphate buffer solution of pH 7.4 maintained at 37°C under mild agitation using a magnetic stirrer. At predefined specific time intervals, aliquots of 1 mL were withdrawn and immediately maintained with the same volume of fresh phosphate buffer solution. The amount of drug released was estimated by taking the absorbance at 260 nm using a UV-Visible Spectrophotometer.

4.3.5.3 Standard curve for gentamicin sulfate (G-S)

The serial dilution was used to prepare the standard solutions of G-S in the concentration range of 05-30 µg/mL in PBS maintained at pH 7.4. Optical absorbance of the resultant solutions was recorded using UV-Visible Spectrophotometer at 260 nm and the calibration curve was plotted between concentration and absorbance (*Figure 4.2*).

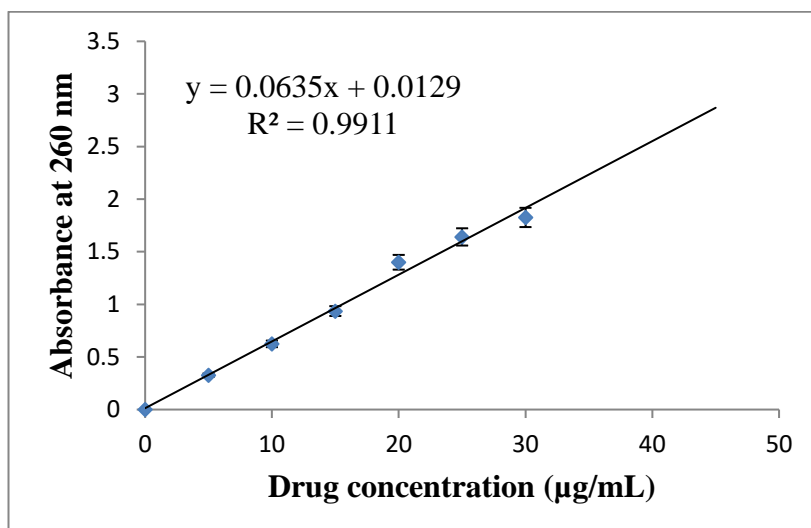


Figure 4.2: Calibration curve of gentamicin sulfate (G-S) in PBS (pH 7.4)

4.3.6 Antimicrobial assessment

E. coli cells were grown at 37°C for 24 h in LB media. Cell number was determined by using a hemocytometer and agar plate counting method and adjusted to 1.5×10^8 CFU/mL. Different concentrations of G-S were used to analyse the antimicrobial property.

4.3.7 Determination of minimum inhibitory concentration (MIC) of gentamicin sulfate (G-S)

The MIC of G-S was determined by the broth dilution method [59]. 1 mL of 1.5×10^8 CFU/mL of *E. coli* in LB broth was taken in 2 mL eppendorf tubes. Different concentrations of G-S (0.10, 0.12, 0.14, 0.16, 0.18, 0.20, 0.22, 0.24 µg/mL) were then added to the eppendorf tubes. The tube containing LB broth and test organism (without G-S) served as the positive control, while the tube containing only LB broth served as the negative control. The capped tubes were then incubated with constant shaking at 37°C for 24 h. After incubation, the broth was streaked onto a sterile nutrient agar plate and again incubated at 37°C for 24 h, and the nutrient agar plate was examined for the

absence of visual colonies for the minimum G-S concentration. The sample in the eppendorf tubes was tested spectrophotometrically for visible turbidity at 600 nm to verify the authenticity of the MIC test.

4.3.8 Determination of minimum biofilm inhibitory concentration (MBIC) of G-S and E-G-S

To determine the MBIC value of G-S different concentrations (2, 5, 10, 15, 20, 25, 30 $\mu\text{g/mL}$) of G-S were used. The EID pieces of [(0.5 \times 0.5) cm^2] containing 24 h grown biofilm were washed thrice and incubated at 37°C for 24 h along with positive control samples (without G-S). After incubation, the EID pieces were analysed for biofilm quantification by the crystal violet assay method described earlier. The spectrophotometric absorbance at 600 nm for biofilm was compared with a positive control to find out the MBIC values. Each MBIC experiment was conducted simultaneously with MIC determination to reduce the error. Same procedure is repeated with E-G-S for assessing its MBIC.

4.4 Results and discussion

4.4.1 Biofilm formation and quantification

The formation of biofilm is not uniform among the EIDs. Variation of biofilm formation with time is shown in *Figure 4.3*. It is seen that the maximum biofilm formation occurred over rubber (latex rubber) and Foley urethral (silicone rubber) catheter after 48 h of incubation while over the enteral feeding and endotracheal (polyurethane) catheter it occur after 24 h. Crystal violet assay leads to purple staining of the bacterial cells that are attached to the surface, whereas abiotic surfaces are not stained. The rubber catheter has been found to be more susceptible surface for biofilm

formation, and the bacteria show a greater tendency to form the biofilm. The different patterns of biofilm formation over the EIDs surfaces indicate that the bacterial biofilm formation depends on the surface properties like texture, grooves, surface charge, and other surface properties of the EIDs.

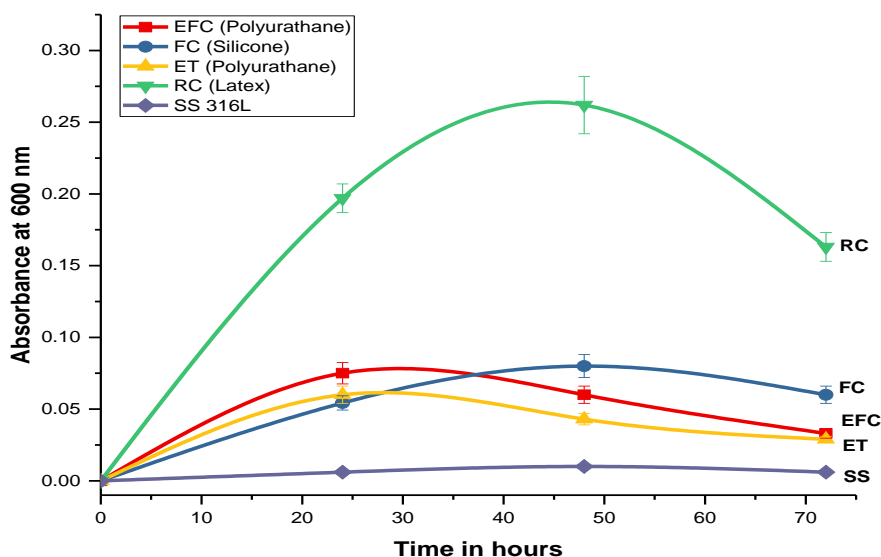


Figure 4.3: Growth of *E. coli* biofilm over different biomaterials

Factors such as hydrophobicity, the surface charge of microorganisms, and material from which catheter is made, size, shape, water contact angle, and topographical features of the surface also play a role in microbial adherence to the catheter surface [60]. The maximum tendency for biofilm formation in the current study occurs over the latex rubber catheter followed by silicone rubber Foley catheter. In both cases, the duration for maximum biofilm formation is 48 h. This may be due to their surface roughness, cracks, and fissure, which is visible in SEM images (*Figure 4.4*).

4.4.2 Physical characteristic of EIDs by SEM

The SEM of EIDs surfaces showed differences in polymer surface structures, cracks, and fissure (*Figure 4.4*). The external surface of latex rubber is more irregular, with grooves (*Figure 4.4a*), thus it provides a better site for microbial attachment and rich biofilm formation (*Figure 4.4b*). Dense rod-shaped *E. coli* bacterial colonies can be visualised on the latex rubber catheter surface. The Foley catheter made of silicone also has surface irregularities (*Figure 4.4c*), but the depressions are not as prominent as in case of rubber catheter. The microbial attachment over the surface is clearly visible (*Figure 4.4d*). The enteral feeding and endotracheal catheter (polyurethane) surface showed the fewest irregularities (*Figure 4.4e, f*) and had few sites available for microbial attachments.

The depressions and irregularities allow the *E. coli* bacteria to grow their colony up to a greater extent as they provide a site for microbial adhesion, and the complex interplay between biofilm matrix and the catheter surface delays the detachment phase of biofilm. In contrast with other catheters, enteral feeding and endotracheal catheters (polyurethane) showed comparatively smoother surfaces with fewer cracks and grooves. Only a few colony forming units (CFU) are seen in SEM images (*Figure 4.4f*), and the maximum biofilm formation occurs after 24 h. It is in accordance with the assumptions that smooth surfaces do not permit easy bacterial attachment. Stainless steel 316L is very smooth, and it hardly provides any bacterial attachment sites. This is why negligible biofilm formation occurred on it.

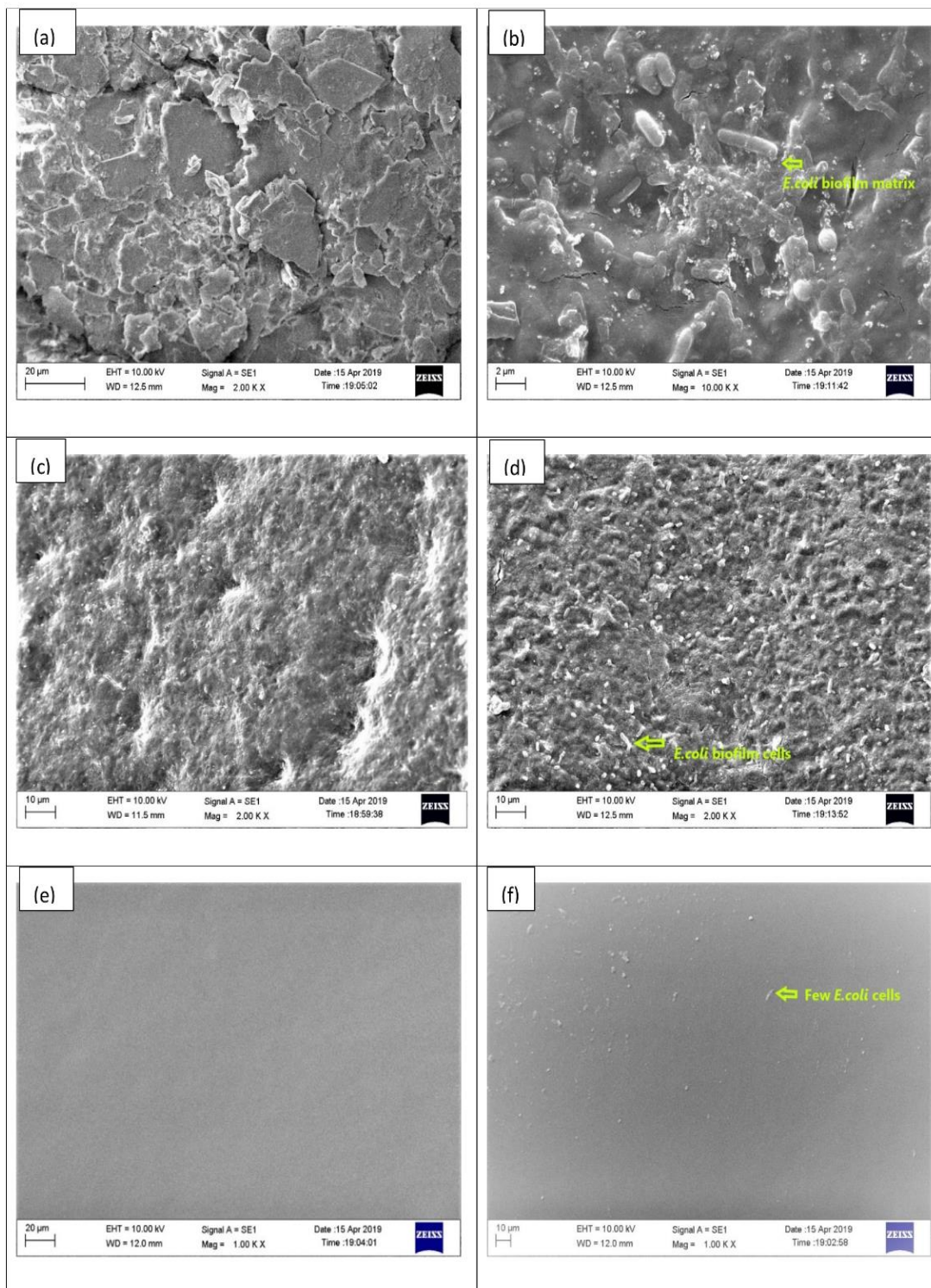
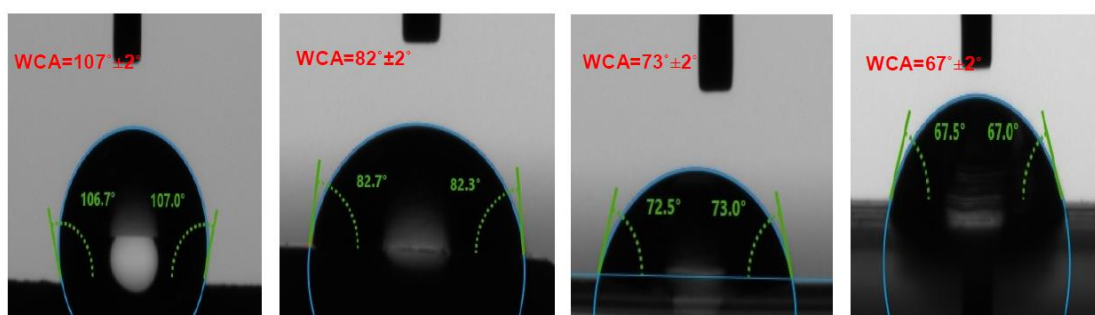


Figure 4.4: SEM images of catheter inner surfaces before and after *E. coli* biofilm formation; (a) Rubber catheter; (b) Biofilm over rubber catheter; (c) Foley catheter; (d) Biofilm over Foley catheter; (e) Endotracheal catheter; (f) Biofilm over endotracheal catheter.

4.4.3 Water contact angle (WCA)

The hydrophilic and hydrophobic properties of the surfaces of the EIDs were analysed with the help of sessile water drop contact angles. The surface with a water contact angle (WCA) $< 90^\circ$ is considered hydrophilic while the surface with WCA $> 90^\circ$ considered hydrophobic. The latex rubber catheter surface is hydrophobic while the Foley catheter (silicone rubber) and the endotracheal tube and enteral feeding catheter made of polyurethane surfaces are hydrophilic (Figure 4.5a-c). The stainless steel (SS 316L) plate used for the biomedical application also showed hydrophilic nature (Figure 4.5d). Considering the nature of the surfaces and WCA, the order of hydrophilic nature is SS 316L $>$ polyurethane $>$ silicone rubber $>$ latex rubber and the same is the order for *E. coli* biofilm formation over the specimens suggesting the possible interdependence between the nature of the material and biofilm formation apart from the other physical factors.



(a) Latex rubber (b) Silicone rubber (c) Polyurethane (d) SS 316L

Figure 4.5: Contact angle of sessile water drop over different catheter surfaces

The water contact angle analysis reveals that increase in hydrophilicity of EID surfaces has a direct relation with the biofilm formation, i.e., moderate hydrophobic biomaterial surfaces provide a better site for microbial proliferation and the hydrophilic biomaterial surfaces are less prone to biofilm formation. This finding is in accordance

with Yue et al. [61]. Recently superhydrophobic surfaces are reported for reduced bacterial adhesion due to the maintenance of entrapped air between the liquid and solid surface by reducing interface contact area and adhesion forces [61]. This reduction in adhesion forces results in easy detachment of bacterial cells. However, if the entrapped air are intruded by the bacterial media, then the roughness and increased effective attachment area result in adherence of more bacterial cells leading to prominent bacterial colonies [62]. The negatively charged bacterial surface also plays a role for the bacterial attachment; the more positive the charge of the surface, the greater the tendency of the microbe for surface attachment [60].

4.4.4 Physical characteristic of Eudragit-RL100 nanoparticle encapsulated gentamicin sulfate (E-G-S)

The SEM image of nanoparticle-encapsulating drugs showed that G-S nanoparticles size was around 100–250 nm (*Figure 4.6a*). The nanoparticles were uniformly distributed. The particle size was analysed through DLS technique and was found in the range of 100–350 nm (*Figure 4.6b*). The size of E-G-S as measured by DLS technique (*Figure 4.6b*) [56] shows that the average hydrodynamic particle diameter is 133.9 ± 40.9 nm in number distribution. The cumulative % distribution of E-G-S from the DLS study reveals that 20% of the particles are below the size of 99.9 nm, 40% are below 109.6 nm, 60% are below 123.6 nm, 80% are below 148.3 nm, 95% are below 202.6 nm.

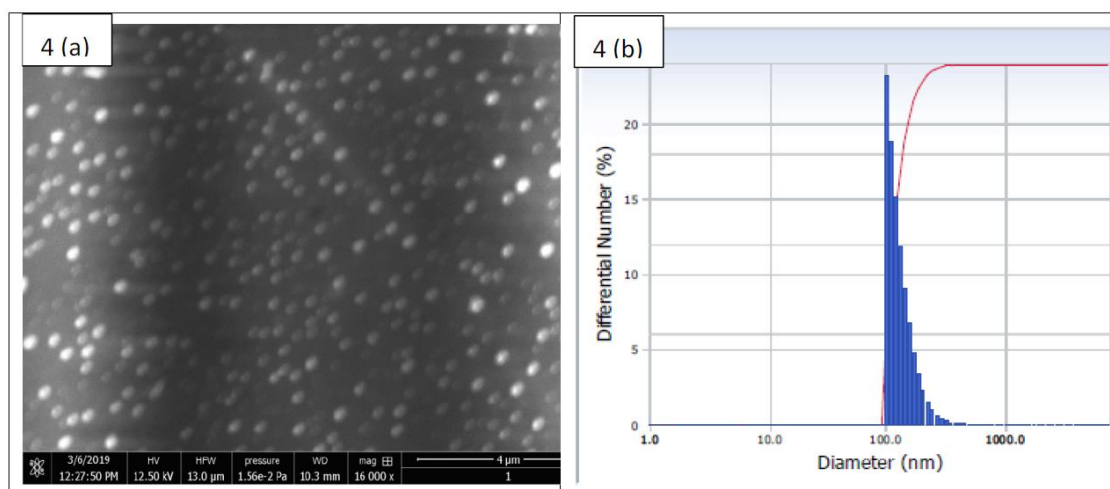


Figure 4.6: Size distribution of Eudragit RL-100 encapsulated gentamicin sulfate (E-G-S) nanoparticles. (a) SEM image; (b) Dynamic light scattering (DLS) measurement of particle size distribution

4.4.4.1 Drug entrapment efficiency

Entrapment experiments conducted with initial G-S concentration of 142.8571 μg/mL indicated that only 100.2256 μg/mL got entrapped in Eudragit RL100 nanoparticles and 42.6315 μg/mL remained untrapped resulting in G-S entrapment efficiency of Eudragit RL-100 to 70.15%. The drug concentration calculations were based on standard equation $Y = 0.065X + 0.0129$ at 260 nm obtained from standard plot of known concentrations (Figure 4.2).

4.4.4.2 *In vitro* G-S release kinetics

In vitro drug release from the nanosuspension in phosphate buffer (pH 7.4) was investigated by the membrane diffusion technique. The sample was taken at regular intervals of 2 h for 24 h. The *in vitro* drug release profile was obtained from the dialysis experiment. Initially, a quick release is seen, probably due to diffusion, but later on, the release slows down and becomes nearly constant after 16 h. More than 70% of the

entrapped drug gets released during this period (*Figure 4.7*). This entrapment efficiency is very good because there is extended-release time up to 16 h, and about 70% of the G-S gets released by that time. Thus, nearly 50% of the initial amount of drug is going to be utilised for the effective biofilm eradication and prevention.

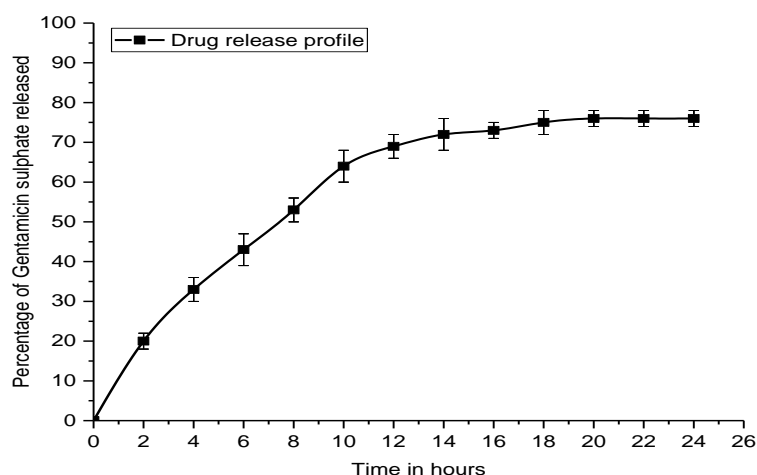


Figure 4.7: Drug release profile of E-G-S in PBS

4.4.5 Minimum inhibitory concentration (MIC) of G-S

The MIC value of G-S for *E. coli* was tested over nutrient agar plates, and the streak pattern of different overnight grown test culture of *E. coli* with a variable concentration of G-S after incubation at 37 °C for 24 h are shown in *Figure 4.8*. On examination of the plate colonies, the growth of *E. coli* was observed up to the concentration of 0.18 µg/mL, but the colony count decreased corresponding to increase of G-S concentration, and no growth was observed at 0.20 and 0.22 µg/mL concentrations. It can be seen that at a G-S concentration above 0.20 µg/mL, the *E. coli* bacteria were unable to grow, thus confirming that the MIC value of G-S for *E. coli*

bacteria is $0.20 \mu\text{g/mL}$. Agar plate method provides qualitative confirmatory test for MIC of G-S.

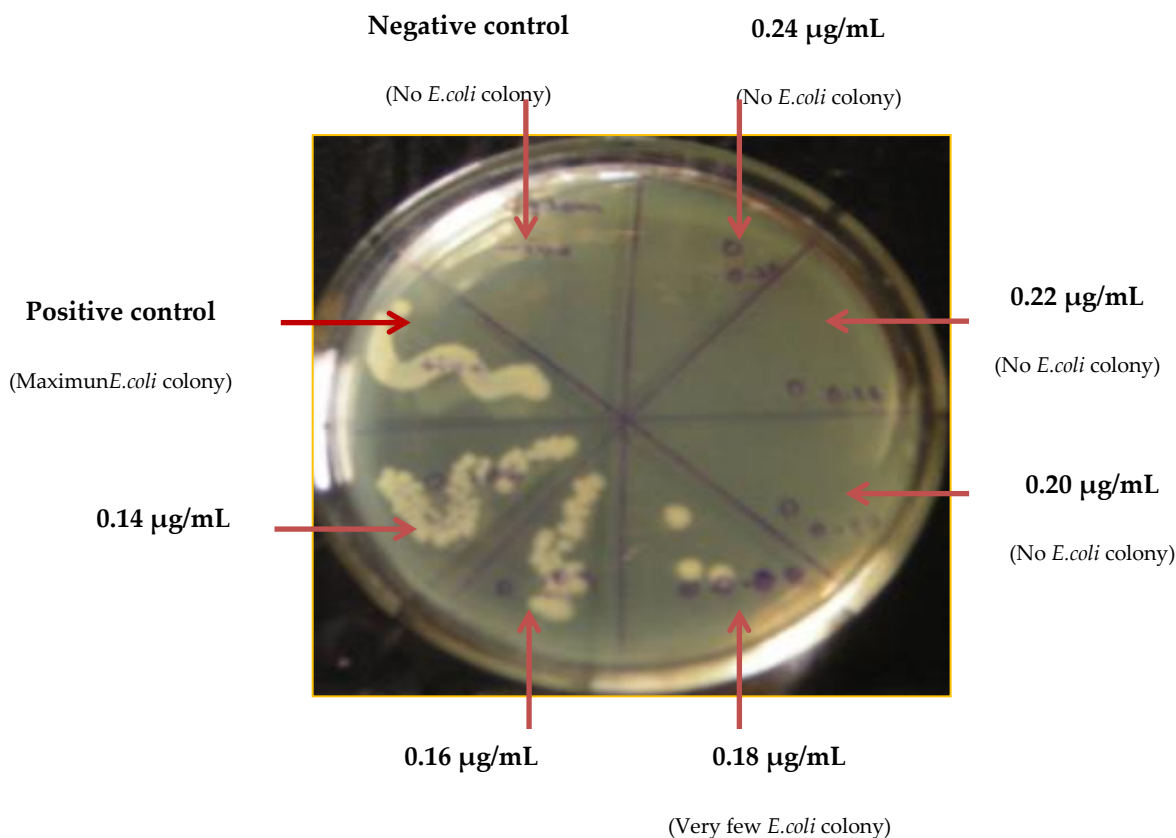


Figure 4.8: Minimum inhibitory concentration (MIC) of G-S for *E. coli* by visual detection of colony forming units (CFU)

4.4.6 Minimum biofilm inhibitory concentration (MBIC) of G-S

Biofilms are structured communities that are unable to show any explanatory drug resistance by any single mechanism, and complete reduction or inhibition is difficult to achieve [35]. MBIC is the lowest concentration of drug that can reduce the microbial biofilm by 50% (MBIC₅₀) or 90% (MBIC₉₀). Based on the percentage reduction in spectrophotometric absorbance at 600 nm, MBIC₅₀ for G-S in the case of the rubber, Foley, and enteral feeding catheters were found to be $20 \mu\text{g/mL}$ (100 times that of

MIC), 10 $\mu\text{g/mL}$ (50 times that of MIC), and 15 $\mu\text{g/mL}$ (75 times that of MIC), respectively, while MBIC_{90} for G-S in the case of the rubber, Foley, and enteral feeding catheters was found to be 30 $\mu\text{g/mL}$ (150 times that of MIC), 20 $\mu\text{g/mL}$ (100 times that of MIC), and 25 $\mu\text{g/mL}$ (125 times that of MIC), respectively (Figure 4.9). It is seen that the MBIC value for EIDs is much higher compared to MIC value under similar conditions for the planktonic *E. coli*. The results demonstrated that in case of sessile microbial biofilm, the drug added was not fully available to the microbes, and a major portion of drug/antimicrobial agent generally reacted and inactivated by chemicals or enzymes of EPS matrix [28]. Polymeric matrix forms a physical barrier and prevents drug penetration, thus protecting sessile microorganisms from being killed [42]. The adaptation acquired by bacterial cells in the biofilm makes it difficult for the antibiotic to act over the biofilm bacterial colonies.

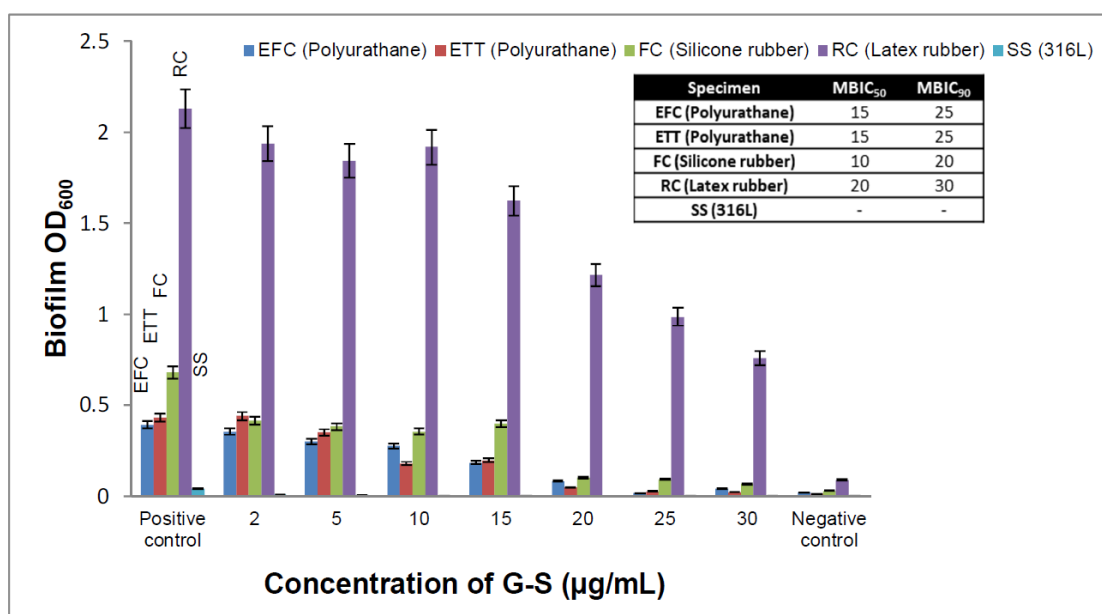


Figure 4.9: Biofilm inhibition pattern over different externally implanted medical devices (EIDs) with G-S

4.4.7 MBIC of Eudragit RL100 nanoparticle-encapsulated G-S (E-G-S)

The MBIC₅₀ and MBIC₉₀ values were calculated for E-G-S, which was used against biofilm in this study. The values for MBIC₅₀ for the nanoparticle-mediated drug delivery for latex, silicone, and polyurethane catheters were found to be 2.5, 2.0, and 1.5 µg/mL, respectively. These concentrations are very low when compared to those of normal untrapped antibiotics (*Figure 4.9*). Similarly, the values for MBIC₉₀ for the E-G-S over latex, silicone, and polyurethane were found to be 4.0, 3.5, and 3.5 µg/mL, respectively (*Figure 4.10*). These concentrations are very much lower than those for untrapped antibiotics. E-G-S MBIC₅₀ and MBIC₉₀ were about 8 and 25 times lower than respective MBIC for untrapped G-S for latex (rubber catheter), 5 and 6 times lower for silicone (Foley catheter) and 15 and 7 times lower for polyurethane (enteral feeding and endotracheal catheter).

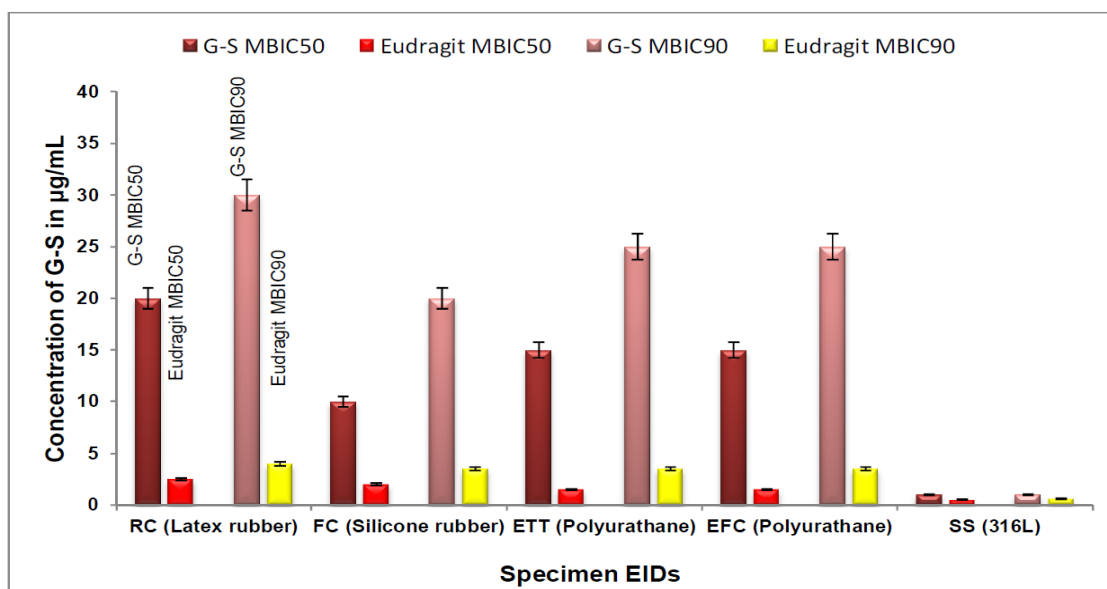


Figure 4.10: Comparison of minimum biofilm inhibitory concentration (MBIC): MBIC₅₀ and MBIC₉₀ for G-S and E-G-S

It is seen that $MBIC_{50}$ and $MBIC_{90}$ of untrapped G-S and E-G-S (Figures 4.9 and 4.10), the latter is 5 to 10 times more efficient in removing the biofilm. A smaller dose of E-G-S will be able to prevent and eradicate biofilm effectively.

Thus, the E-G-S is efficient in preventing and eradicating the biofilm over EIDs and is also safe as it reduces the biological payload of antibiotics. It also helps to reduce the tolerant bacterial infection within the subject's body. E-G-S exhibited enhanced biofilm penetration due to unique size-dependent chemical and physical properties of nanoparticles by virtue of their high surface area to volume ratio. The Eudragit RL-100 swells partially at physiological pH causing prolonged drug release of the encapsulated antibiotic G-S. Further lower doses of the drug are needed as the nanoparticles can easily penetrate the protective EPS due to their size to act directly on the target site without exceeding the systemic toxicity value of the drug (G-S) and preventing possible side effects [63]. Complete removal of formed biofilm is difficult to achieve, but the Eudragit RL-100 nanoparticle-mediated drug delivery can efficiently act against the *E. coli* biofilms. The polymeric biomaterial surfaces are differentially susceptible to microbial colonization based on their surface properties, and E-G-S nanoparticles offer a better perspective for catheter-associated biofilm removal.

4.5 Conclusion

Material characteristics and surface properties are directly related to microbial adhesion, colonisation and detachment. Irregularities on the surface promote biofilm formation because of the increased effective surface area for microbial attachment. The rough surfaces and depressions in the uneven surfaces provide shelter and site for microbial colonisation. *In vitro* studies have confirmed that both adherence of biofilm and decrease in hydrophilicity increase in the order: Stainless steel 316L < polyurethane

< silicone < latex for Gram-negative *E. coli*. The E-G-S nanopowder has better protective property against the biofilm, so its coating or its powdered form is very effective against prevention of biofilm-related infections either iatrogenic or wound related. The study also confirms that the hydrophobic surfaces in the moderate range are more prone to bacterial cell attachment and biofilm formation, and the tendency to form biofilm over the material decreases with an increase in hydrophilicity. The polyurethane polymer is found to be most suitable for the EIDs as compared to silicone and latex rubber.

Reference

- [1] Y. Dhar, Y. Han, Current developments in biofilm treatments : Wound and implant infections, *Eng. Regen.* 1 (2020) 64–75.
- [2] R.A. Mendoza, J.-C. Hsieh, R.D. Galiano, *The Impact of biofilm formation on wound healing*, 2019.
- [3] G. Zhao, M.L. Usui, S.I. Lippman, G.A. James, P.S. Stewart, P. Fleckman, J.E. Olerud, Biofilms and inflammation in chronic wounds, *Adv. Wound Care.* 2 (2013) 389–399.
- [4] M. Abrigo, S.L. McArthur, P. Kingshott, Electrospun nanofibers as dressings for chronic wound care: Advances, challenges, and future prospects, *Macromol. Biosci.* 14 (2014) 772–792.
- [5] Y.-H. Yen, C.-M. Pu, C.-W. Liu, Y.-C. Chen, Y.-C. Chen, C.-J. Liang, J.-H. Hsieh, H.-F. Huang, Y.-L. Chen, Curcumin accelerates cutaneous wound healing via multiple biological actions: The involvement of TNF- α , MMP-9, α -SMA, and collagen, *Int. Wound J.* 15 (2018) 605–617.
- [6] P. Das Ghatak, S.S. Mathew-Steiner, P. Pandey, S. Roy, C.K. Sen, A surfactant polymer dressing potentiates antimicrobial efficacy in biofilm disruption, *Sci. Rep.* 8 (2018) 1–9.
- [7] J. Treter, a J. Macedo, Catheters: a suitable surface for biofilm formation, *Sci. against Microb. Pathog. Commun. Curr. Res. Technol. Adv.* (2011) 835–842.
- [8] Z. Khatoon, C.D. McTiernan, E.J. Suuronen, T.F. Mah, E.I. Alarcon, Bacterial biofilm formation on implantable devices and approaches to its treatment and prevention, *Heliyon.* 4 (2018).
- [9] J.S. VanEpps, J.G. Younger, Implantable device-related infection., *Shock.* 46 (2016) 597–608.
- [10] C. Sousa, M. Henriques, R. Oliveira, Mini-review: Antimicrobial central venous catheters - recent advances and strategies, *Biofouling.* 27 (2011) 609–620.
- [11] C. De La Fuente-Núñez, F. Reffuveille, S.C. Mansour, S.L. Reckseidler-Zenteno, D. Hernández, G. Brackman, T. Coenye, R.E.W. Hancock, D-enantiomeric peptides that eradicate wild-type and multidrug-resistant biofilms and protect against lethal *Pseudomonas aeruginosa* infections, *Chem. Biol.* 22 (2015) 196–205.
- [12] D. Lebeaux, J.-M. Ghigo, C. Beloin, Biofilm-related Infections: Bridging the gap between clinical management and fundamental aspects of recalcitrance toward antibiotics, *Microbiol. Mol. Biol. Rev.* 78 (2014) 510–543.
- [13] U. Römling, C. Balsalobre, Biofilm infections, their resilience to therapy and innovative treatment strategies, *J. Intern. Med.* 272 (2012) 541–561.

- [14] C. Cattò, F. Cappitelli, Testing anti-biofilm polymeric surfaces: Where to start?, *Int. J. Mol. Sci.* 20 (2019) 3794.
- [15] Carinci, Lauritano, Bignozzi, Pazzi, Candotto, Santos de Oliveira, Scarano, A New strategy against peri-Implantitis: Antibacterial internal coating, *Int. J. Mol. Sci.* 20 (2019) 3897.
- [16] M.M. Querido, L. Aguiar, P. Neves, C.C. Pereira, J.P. Teixeira, Self-disinfecting surfaces and infection control, *Colloids Surfaces B Biointerfaces.* 178 (2019) 8–21.
- [17] M. Vallet-Regí, B. González, I. Izquierdo-Barba, Nanomaterials as promising alternative in the infection treatment, *Int. J. Mol. Sci.* 20 (2019) 3806.
- [18] E. Caló, V. V. Khutoryanskiy, Biomedical applications of hydrogels: A review of patents and commercial products, *Eur. Polym. J.* 65 (2015) 252–267.
- [19] C. Han, N. Romero, S. Fischer, J. Dookran, A. Berger, A.L. Doiron, Recent developments in the use of nanoparticles for treatment of biofilms, *Nanotechnol. Rev.* 6 (2017) 383–404.
- [20] K. Ikuma, A.W. Decho, B.L.T. Lau, When nanoparticles meet biofilms - Interactions guiding the environmental fate and accumulation of nanoparticles, *Front. Microbiol.* 6 (2015) 1–6.
- [21] M. Emer, M.B. Cardoso, Biomolecular corona formation: Nature and bactericidal impact on surface-modified silica nanoparticles, *J. Mater. Chem. B.* 5 (2017) 8052–8059.
- [22] S. Das, P.K. Suresh, R. Desmukh, Design of Eudragit RL 100 nanoparticles by nanoprecipitation method for ocular drug delivery, *Nanomedicine Nanotechnology, Biol. Med.* 6 (2010) 318–323.
- [23] D. Pavithra, M. Doble, Biofilm formation, bacterial adhesion and host response on polymeric implants - Issues and prevention, *Biomed. Mater.* 3 (2008).
- [24] S.L. Percival, L. Suleman, C. Vuotto, G. Donelli, Healthcare-associated infections, medical devices and biofilms: Risk, tolerance and control, *J. Med. Microbiol.* 64 (2015) 323–334.
- [25] Y. Xu, L.H. Larsen, J. Lorenzen, L. Hall-Stoodley, J. Kikhney, A. Moter, T.R. Thomsen, Microbiological diagnosis of device-related biofilm infections, *APMIS.* 125 (2017) 289–303.
- [26] Y.M. Wi, R. Patel, Understanding biofilms and novel approaches to the diagnosis, prevention, and treatment of medical device-associated infections, *Infect. Dis. Clin. North Am.* 32 (2018) 915–929.
- [27] D. Lebeaux, A. Chauhan, O. Rendueles, C. Beloin, From *in vitro* to *in vivo* models of bacterial biofilm-related infections, *Pathogens.* 2 (2013) 288–356.
- [28] G. Gebreyohannes, A. Nyerere, C. Bii, D.B. Sbhatu, Challenges of intervention,

- treatment, and antibiotic resistance of biofilm-forming microorganisms, *Heliyon*. 5 (2019) e02192.
- [29] B. Parrino, D. Schillaci, I. Carnevale, E. Giovannetti, P. Diana, G. Cirrincione, S. Cascioferro, Synthetic small molecules as anti-biofilm agents in the struggle against antibiotic resistance, *Eur. J. Med. Chem.* 161 (2019) 154–178.
- [30] H. Koo, R.N. Allan, R.P. Howlin, P. Stoodley, L. Hall-Stoodley, Targeting microbial biofilms: Current and prospective therapeutic strategies, *Nat. Rev. Microbiol.* 15 (2017) 740–755.
- [31] O. Constantinescu, N. Sahnazarov, A. Muțiu, Quorum Sensing in Bacteria: the LuxR-LuxI Family of Cell Density-Responsive Transcriptional Regulators, *J. Bacteriol.* 176 (1994) 269–275.
- [32] T. Ishida, T. Ikeda, N. Takiguchi, A. Kuroda, H. Ohtake, J. Kato, Inhibition of quorum sensing in *Pseudomonas aeruginosa* by N-acyl cyclopentylamides, *Appl. Environ. Microbiol.* 73 (2007) 3183–3188.
- [33] K.P. Miller, L. Wang, Y.P. Chen, P.J. Pellechia, B.C. Benicewicz, A.W. Decho, Engineering nanoparticles to silence bacterial communication, *Front. Microbiol.* 6 (2015) 1–7.
- [34] R. Nijland, M.J. Hall, J. Grant Burgess, Dispersal of biofilms by secreted, matrix degrading, Bacterial DNase, *PLoS One*. 5 (2010).
- [35] C. De la Fuente-Núñez, F. Reffuveille, L. Fernández, R.E.W. Hancock, Bacterial biofilm development as a multicellular adaptation: Antibiotic resistance and new therapeutic strategies, *Curr. Opin. Microbiol.* 16 (2013) 580–589.
- [36] M.A. Díaz De Rienzo, P.S. Stevenson, R. Marchant, I.M. Banat, *Pseudomonas aeruginosa* biofilm disruption using microbial surfactants, *J. Appl. Microbiol.* 120 (2016) 868–876.
- [37] A.P. Desbois, V.J. Smith, Antibacterial free fatty acids: Activities, mechanisms of action and biotechnological potential, *Appl. Microbiol. Biotechnol.* 85 (2010) 1629–1642.
- [38] K.S. Brandenburg, K.J. Rodriguez, J.F. McAnulty, C.J. Murphy, N.L. Abbott, M.J. Schurr, C.J. Czuprynski, Tryptophan inhibits biofilm formation by *Pseudomonas aeruginosa*, *Antimicrob. Agents Chemother.* 57 (2013) 1921–1925.
- [39] J. Kim, W. Park, Indole: a signaling molecule or a mere metabolic byproduct that alters bacterial physiology at a high concentration?, *J. Microbiol.* 53 (2015) 421–428.
- [40] E. Banin, K.M. Brady, E.P. Greenberg, Chelator-induced dispersal and killing of *Pseudomonas aeruginosa* cells in a biofilm, *Appl. Environ. Microbiol.* 72 (2006) 2064–2069.
- [41] F. Schreiber, M. Beutler, D. Enning, M. Lamprecht-Grandio, O. Zafra, J.

- González-Pastor, D. De Beer, The role of nitric-oxide-synthase-derived nitric oxide in multicellular traits of *Bacillus subtilis* 3610: Biofilm formation, swarming, and dispersal, *BMC Microbiol.* 11 (2011).
- [42] A. Algburi, N. Comito, D. Kashtanov, L.M.T. Dicks, M.L. Chikindas, Control of biofilm formation: Antibiotics and beyond, *Appl. Environ. Microbiol.* 83 (2017) 1–16.
- [43] L. Zhang, E. Liang, Y. Cheng, T. Mahmood, F. Ge, K. Zhou, M. Bao, L. Lv, L. Li, J. Yi, C. Lu, Y. Tan, Is combined medication with natural medicine a promising therapy for bacterial biofilm infection?, *Biomed. Pharmacother.* 128 (2020).
- [44] B. Gumus, T. Acar, T. Atabey, S. Derman, F. Sahin, T. Arasoglu, The battle against biofilm infections: juglone loaded nanoparticles as an anticandidal agent, *J. Biotechnol.* 316 (2020) 17–26.
- [45] Y. Qiu, D. Xu, G. Sui, D. Wang, M. Wu, L. Han, H. Mu, J. Duan, Gentamicin decorated phosphatidylcholine-chitosan nanoparticles against biofilms and intracellular bacteria, *Int. J. Biol. Macromol.* 156 (2020) 640–647.
- [46] P. Guo, B.A. Buttaro, H.Y. Xue, N.T. Tran, H.L. Wong, Lipid-polymer hybrid nanoparticles carrying linezolid improve treatment of methicillin-resistant *Staphylococcus aureus* (MRSA) harbored inside bone cells and biofilms, *Eur. J. Pharm. Biopharm.* 151 (2020) 189–198.
- [47] Y. Liu, P.C. Naha, G. Hwang, D. Kim, Y. Huang, A. Simon-Soro, H.I. Jung, Z. Ren, Y. Li, S. Gubara, F. Alawi, D. Zero, A.T. Hara, D.P. Cormode, H. Koo, Topical ferumoxytol nanoparticles disrupt biofilms and prevent tooth decay *in vivo* via intrinsic catalytic activity, *Nat. Commun.* 9 (2018) 2920.
- [48] F. Kong, J. Wang, R. Han, S. Ji, J. Yue, Y. Wang, L. Ma, Antifungal Activity of Magnesium Oxide Nanoparticles: Effect on the Growth and Key Virulence Factors of *Candida albicans*, *Mycopathologia.* 185 (2020) 485–494.
- [49] D. Ranmadugala, A. Ebrahiminezhad, M. Manley-Harris, Y. Ghasemi, A. Berenjian, The effect of iron oxide nanoparticles on *Bacillus subtilis* biofilm, growth and viability, *Process Biochem.* 62 (2017) 231–240.
- [50] P.C. Naha, Y. Liu, G. Hwang, Y. Huang, S. Gubara, V. Jonnakuti, A. Simon-Soro, D. Kim, L. Gao, H. Koo, D.P. Cormode, Dextran-Coated Iron Oxide Nanoparticles as Biomimetic Catalysts for Localized and pH-Activated Biofilm Disruption, *ACS Nano.* 13 (2019) 4960–4971.
- [51] B.S. Vasile, A.C. Birca, M.C. Musat, A.M. Holban, Wound dressings coated with silver nanoparticles and essential oils for the management of wound infections, *materials (Basel).* 13 (2020) 1682.
- [52] E. Bhatia, R. Banerjee, Hybrid silver-gold nanoparticles suppress drug resistant polymicrobial biofilm formation and intracellular infection, *J. Mater. Chem. B.* 8 (2020) 4890–4898.

- [53] G.A. O'Toole, Microtiter Dish Biofilm Formation Assay, *J. Vis. Exp.* (2011).
- [54] D. Djordjevic, M. Wiedmann, L.A. McLandsborough, Microtiter plate assay for assessment of *Listeria monocytogenes* biofilm formation, *Appl. Environ. Microbiol.* 68 (2002) 2950–2958.
- [55] K. Doll, K.L. Jongstaphongpun, N.S. Stumpp, A. Winkel, M. Stiesch, Quantifying implant-associated biofilms: Comparison of microscopic, microbiologic and biochemical methods, *J. Microbiol. Methods.* 130 (2016) 61–68.
- [56] J. Lim, S.P. Yeap, H.X. Che, S.C. Low, Characterization of magnetic nanoparticle by dynamic light scattering, *Nanoscale Res. Lett.* 8 (2013) 1–14.
- [57] G. Ajmal, G.V. Bonde, P. Mittal, G. Khan, V.K. Pandey, B. V. Bakade, B. Mishra, Biomimetic PCL-gelatin based nanofibers loaded with ciprofloxacin hydrochloride and quercetin: A potential antibacterial and anti-oxidant dressing material for accelerated healing of a full thickness wound, *Int. J. Pharm.* 567 (2019) 118480.
- [58] R.O. Salama, D. Traini, H.K. Chan, P.M. Young, Preparation and characterisation of controlled release co-spray dried drug-polymer microparticles for inhalation 2: Evaluation of in vitro release profiling methodologies for controlled release respiratory aerosols, *Eur. J. Pharm. Biopharm.* 70 (2008) 145–152.
- [59] I. Wiegand, K. Hilpert, R.E.W. Hancock, Agar and broth dilution methods to determine the minimal inhibitory concentration (MIC) of antimicrobial substances, *Nat. Protoc.* 3 (2008) 163–175.
- [60] K.G. Neoh, M. Li, E.T. Kang, E. Chiong, P.A. Tambyah, Surface modification strategies for combating catheter-related complications: recent advances and challenges, *J. Mater. Chem. B.* 5 (2017) 2045–2067.
- [61] Y. Yuan, M.P. Hays, P.R. Hardwidge, J. Kim, Surface characteristics influencing bacterial adhesion to polymeric substrates, *RSC Adv.* 7 (2017) 14254–14261.
- [62] E.J. Falde, S.T. Yohe, Y.L. Colson, M.W. Grinstaff, Superhydrophobic materials for biomedical applications, *Biomaterials.* 104 (2016) 87–103.
- [63] P. Gao, X. Nie, M. Zou, Y. Shi, G. Cheng, Recent advances in materials for extended-release antibiotic delivery system, *J. Antibiot. (Tokyo).* 64 (2011) 625–634.